

Diffusion-controlled formation mechanism of dual-phase structure during Al induced crystallization of SiGe

Tian-Wei Zhang,¹ Fei Ma,^{1,2,a)} Wei-Lin Zhang,¹ Da-Yan Ma,¹ Ke-Wei Xu,^{1,3,a)} and Paul K. Chu^{2,a)}

¹State Key Laboratory for Mechanical Behavior of Materials, Xi'an Jiaotong University, Xi'an 710049, Shaanxi, China

²Department of Physics and Materials Science, City University of Hong Kong, Tat Chee Avenue, Kowloon, Hong Kong, China

³Department of Physics and Opt-electronic Engineering, Xi'an University of Arts and Science, Xi'an 710065, Shaanxi, China

(Received 10 March 2011; accepted 30 January 2012; published online 15 February 2012)

Aluminum induced crystallization of amorphous SiGe at low temperature is studied and a dual-phase stacked structure with different compositions emerges when the annealing temperature is higher than a critical value. This behavior is very sensitive to the oxidization state of the interlayer. A model based on energetics is proposed to elucidate this temperature dependent behavior. Thermodynamically, it can be ascribed to the competition between grain-boundary-mediated and interface-mediated crystallization and kinetically, it stems from the different diffusion rates of Si and Ge. The results are useful to the design and fabrication of high-efficiency solar cells. © 2012 American Institute of Physics. [doi:10.1063/1.3685712]

Polycrystalline silicon-germanium (poly-SiGe) is attracting more attention in the field of solar cells because of its higher photoelectric conversion efficiency.^{1,2} SiGe thin films fabricated by vapor deposition are typically amorphous, and efficient crystallization on inexpensive substrates such as glass at a low temperature is crucial to low-cost and energy-saving production. Metal induced crystallization (MIC) has recently been studied in amorphous Si³⁻⁷ and SiGe alloy.^{8,9} Atom diffusion is believed to play an important role in the MIC process which may be complicated in the SiGe binary system due to the different diffusion characteristics of Si and Ge. In this work, the phase structures during Al-induced crystallization of amorphous SiGe are studied from the viewpoint of thermodynamics and kinetics.

Bi-layered Al/a-Si_{1-x}Ge_x thin films with an equal thickness of 200 nm and Ge composition of about 35% were fabricated on glass substrates by RF magnetron sputtering at room temperature. After Al deposition, the samples were exposed to air for 1 s, 3 min, or 3 h to investigate the influence of the oxide interlayer. The samples were subsequently annealed under dry N₂ for 150 min at different temperatures from 250 °C to 400 °C. Fig. 1 displays the representative x-ray diffraction patterns of the samples without the oxide interlayer. Only the Al (111) diffraction peak can be observed from the as-deposited sample indicating an amorphous state in the original SiGe. After annealing at 250 °C, three diffraction peaks, namely (111), (220), and (311), can be observed at 2θ of 28°, 46°, and 55° indicating crystallization of a-SiGe. If the annealing temperature is raised to 300 °C, double peaks appear unexpectedly between the diffraction peaks of single-crystal Si and Ge, indicating the formation of a dual-phase structure. It is also found that the crystallization temperature and dual-phase formation temper-

ature increase to 275 °C and 325 °C, respectively, for the sample exposed to air for 1 s after Al deposition. If the air exposure time is prolonged to 3 min, they are increased to the same value of about 350 °C but do not change further with longer air exposure time.

Grain boundary (GB) mediated¹⁰ and interface mediated mechanisms have been proposed to explain Al-induced crystallization of amorphous Si/Ge.¹¹ The former involves interdiffusion of Si/Ge atoms into the Al grain boundaries and crystallization there. In comparison, crystallization occurs directly at the interface of Al and amorphous Si/Ge in the latter case. Figs. 2(a) and 2(b) depict the optical images of the samples without the oxide interlayer obtained from the backside of the transparent glass substrate. In the sample annealed at 250 °C, about 90 grains can be observed within the field of view covering 32% of the area, whereas about 101 grains covering 41% of the whole area are observed from the 350 °C annealed sample. These SiGe dendrites are

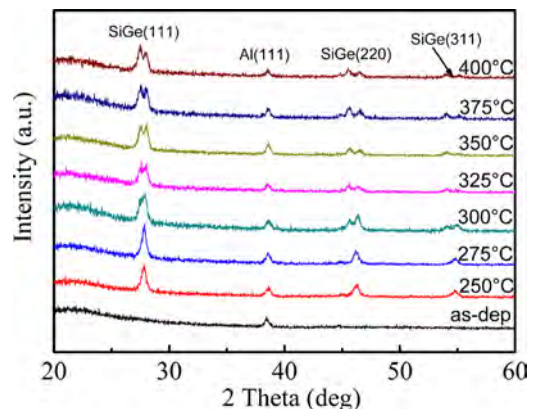


FIG. 1. (Color online) XRD patterns of the Al/a-SiGe samples without an oxide interlayer (as-deposited and annealed at different temperature from 250 °C to 400 °C).

^{a)} Authors to whom correspondence should be addressed. Electronic addresses: mafei@mail.xjtu.edu.cn, kwxu@mail.xjtu.edu.cn, and paul.chu@cityu.edu.hk.

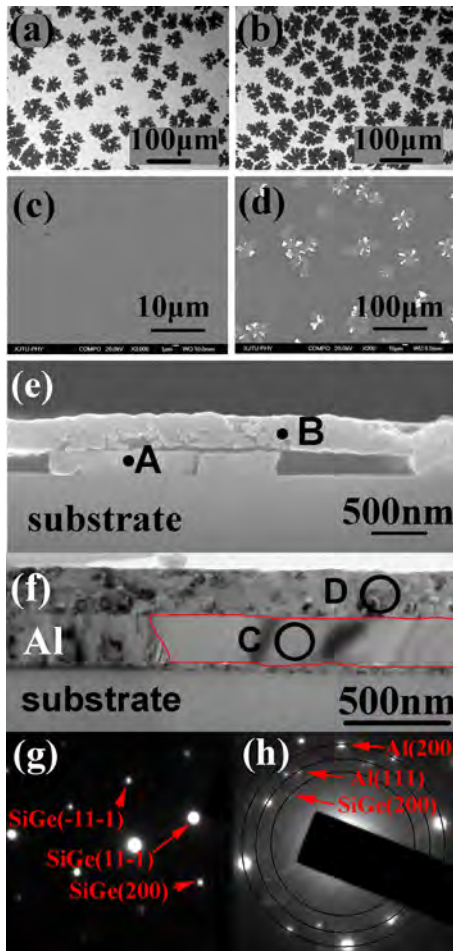


FIG. 2. (Color online) Optical micrographs acquired from the backside of the samples without an oxide interlayer annealed at (a) 250 °C and (b) 350 °C with the bright and dark areas corresponding to aluminum and c-SiGe; SEM micrographs of the sample annealed at (c) 250 °C and (d) 350 °C; (e) Cross-sectional SEM and (f) TEM micrographs of the sample with oxide interlayer annealed at 350 °C; electron diffraction patterns of (g) region C and (h) region D.

grown from the initial Al sublayer in accordance with GB-mediated crystallization. The scanning electron microscopy (SEM, JEOL JSM-7000F) pictures in Figs. 2(c) and 2(d) disclose that different from the smooth surface of the sample annealed at 250 °C, large dendrites tens of micrometers in diameters emerge from the surface of the sample annealed at 350 °C. It indicates another crystallization mechanism. That is, SiGe grains nucleate at the Al/SiGe interface and grow gradually on the surface according to interface-mediated crystallization. Fig. 2(e) displays the cross-sectional SEM image of the sample without an oxide interlayer annealed at 350 °C after Al has been removed by wet chemical etching in hot hydrochloric acid (HCl). The grains denoted by A and B are crystallized SiGe in the initial Al and a-SiGe sublayers, respectively, corresponding to the dendrites displayed in Figs. 2(b) and 2(d). These grains can also be found from regions C and D in Fig. 2(f) and further confirmed by the electron diffraction patterns (HR-TEM, JEOL JEM-2010) in Figs. 2(g) and 2(h). Energy-dispersive x-ray spectroscopy (EDS) reveals that the Ge fraction is 40.7 at. % at point A and 33.2 at. % at point B. Hence, the chemical compositions of the SiGe grains formed in the initial Al and SiGe sublayers are different. The lattice constant of the SiGe alloy

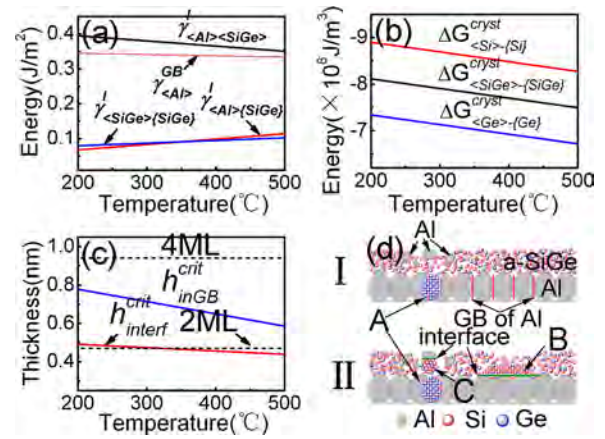


FIG. 3. (Color online) (a) Calculated interface Gibbs free energies, (b) bulk crystallization energies, and (c) critical thickness required for crystallization and thickness of activated regions with $\langle \rangle$ representing the crystalline phase, $\{ \}$ the amorphous phase, and γ_{ij}^I Gibbs free energy of the i and j interface. (d) Schematic diagram of crystallization mechanism at a temperature below (panel I) or above (panel II) the critical value.

grains should differ from each other, consequently spurring the dual-phase structure.

Thermodynamically, metal induced crystallization is driven by the minimization of Gibbs free energy. In GB-mediated crystallization, two interfaces of Al/c-SiGe (crystalline SiGe) are formed instead of two interfaces of Al/a-SiGe. On the other hand, in interface-mediated crystallization, two different interfaces are produced, namely Al/c-SiGe and a-SiGe/c-SiGe. The average energy of Si and Ge is used as the approximate value for SiGe and the interface energies of Al/c-SiGe, Al/a-SiGe, and a-SiGe/c-SiGe can be determined by thermodynamics.^{11,12} The trend as a function of temperature is illustrated in Fig. 3(a). Compared to the Al/a-SiGe interface, the interface energy of Al/c-SiGe increases greatly thereby preventing crystallization. On the other hand, the bulk Gibbs free energy is reduced due to the orderly arrangement of the atoms, as indicated by the negative values shown in Fig. 3(b) consequently promoting crystallization. The interface free energy and bulk free energy compete to determine whether crystallization takes place or not. Only when enough atoms are involved, that is, the thickness of the activated amorphous layer is larger than a critical value, will the reduced bulk free energy be larger than the increased interface free energy for crystallization to take place spontaneously.^{11,13} This can be described by $\Delta G^{cryst} \bullet V + \Delta \gamma^I \bullet S < 0$, in which ΔG^{cryst} is the reduced bulk free energy in unit volume during crystallization, $\Delta \gamma^I$ is the increased interface free energy per unit area, and V and S are the volume and surface area of crystallized SiGe, respectively. By letting the reduced bulk free energy be equal to the increased interface free energy, we obtain the critical thickness required for crystallization of a-SiGe in the Al grain boundaries and interfaces of Al/a-SiGe. The results are shown in Fig. 3(c). The critical thickness decreases slightly from 0.49 nm at 200 °C to 0.44 nm at 500 °C for the Al/a-SiGe interface, whereas it decreases greatly from 0.78 nm at 200 °C to 0.59 nm at 500 °C for the Al grain boundaries. During the MIC process, only Si and Ge atoms near the metal layers can be activated. As reported previously,¹² the thickness of the activated SiGe layer is about 2 monolayers (ML), that is, 0.44 nm for Si and

0.50 nm for Ge, by taking the average value of 0.47 nm for SiGe. In other words, only these atoms can overcome the energy barrier to crystallize at low temperature. At the Al grain boundaries, a-SiGe layer is sandwiched between two Al grains and the total thickness of the Si and Ge atoms activated by the metal layers is 4 ML which is thicker than the critical thickness required for crystallization at any temperature as shown in Fig. 3(c). However, at the Al/a-SiGe interface, only when the temperature is raised to 320 °C will the critical thickness be reduced to 2 ML in order that interface-mediated crystallization can take place.

Kinetically, the composition evolution is indeed controlled by atomic diffusion as described by Arrhenius equation, $D = D_0 \exp\left[\frac{-Q}{RT}\right]$,¹⁴ where D_0 is the pre-exponential factor, Q is the activation energy, and T and R are the absolute temperature and gas constant, respectively. By substituting $D_0 = 1.38 \times 10^{-5} \text{ m}^2/\text{s}$ and $Q = 117.6 \text{ kJ/mole}$ for Si atoms as well as $D_0 = 4.80 \times 10^{-5} \text{ m}^2/\text{s}$ and $Q = 121.3 \text{ kJ/mole}$ for Ge atoms,¹⁴ the diffusion rate of Ge is found to be about 3.5 times that of Si in this temperature range. Hence, a physical model of the formation of this dual-phase structure can be proposed, as schematically presented in Fig. 3(d). At a temperature below 320 °C, only GB-mediated crystallization can take place and SiGe grains with a single composition might be evidenced there, as indicated by A in panel I of Fig. 3(d); at the same time, some Al atoms diffuse into the initial amorphous SiGe layer and crystallize there. So layer exchange takes place, as displayed in Figure 2(f). When the temperature is raised to a higher value, interface-mediated crystallization also becomes possible, which can take place at the initial Al/SiGe interface as well as near the Al grains formed in the initial amorphous SiGe layer, as indicated by B and C, respectively, in panel II of Fig. 3(d). The crystallized SiGe alloy in the Al GBs should be Ge rich due to its larger diffusion rate, while that near the Al/SiGe interface has a smaller fraction of Ge because of less Ge atoms left. This leads to the dual-phase structure of SiGe that may improve the photocurrent of solar cells but without affecting the open-circuit voltage.¹⁵

The oxide interlayer between Al and SiGe usually acts as a diffusion barrier and affects the crystallization process and dual-phase formation. However, it should be mentioned that at the temperature range between 200 and 500 °C, the oxide interlayer may be broken locally,¹⁶ and an intermixed phase of Al_xSi can be established in the oxide interlayer.¹⁷ Both the “broken” grains and Al_xSi phase may serve as a diffusion path for Al and Si atoms.¹⁸ Al-induced crystallization and dual-phase formation can thus take place but at a smaller velocity and density. Long-time exposure in air may produce a thicker oxide interlayer and so the crystallization temperature and dual-phase formation temperature should be increased depending on the thickness of the oxide interlayer. These two temperatures are close to the constant value observed from samples exposed to air for longer than 3 min. That is to say, 3 min air exposure is sufficient for complete oxidation of the Al surface layer. On the other hand, if the annealing time is prolonged so that more sufficient atoms can diffuse to the Al grains, a dual-phase structure can also be formed in the samples with a thicker oxide interlayer. For instance, 5 h annealing is required for the emergence of the

dual-phase structure after annealing at 300 °C. However, this dual-phase structure disappeared as a result of further atom diffusion driven by chemical potential difference if the annealing time was prolonged to 100 h.⁸

In summary, Al induced crystallization of amorphous SiGe has been studied. A dual phase structure is observed after annealing at temperatures higher than a critical value. Thermodynamic and kinetic studies suggest that only GB-mediated crystallization takes place below the critical temperature, and SiGe grains with a larger Ge fraction are formed due to its higher diffusion rate. At a temperature higher than the critical value, both GB-mediated and interface mediated crystallizations occur, and polycrystalline SiGe in the Al/a-SiGe interface has a smaller Ge concentration compared to that in the Al grain boundaries. Hence, a dual-phase SiGe structure is formed and believed to be useful in high-efficiency solar cells. The critical temperature of dual-phase formation is raised slightly if there is an oxide interlayer between the Al and a-SiGe. This behavior is also time and composition dependent, requiring further research works. The model described here can be extended to metal induced crystallization of other alloy systems.

This work was jointly supported by Key Project of Chinese National Programs for Fundamental Research and Development (Grant No. 2010CB631002), National Natural Science Foundation of China (Grant Nos. 50901057 and 51171145), New Century Excellent Talents in University, National Ministries and Commissions (Grant No. 6139802-04), Fundamental Research Funds for the Central Universities, and Hong Kong Research Grants Council (RGC) General Research Funds (GRF) No. CityU 112510.

¹K. Brunner, *Rep. Prog. Phys.* **65**, 27 (2002).

²A. E. Franke, J. M. Heck, T. J. King, and R. T. Howe, *J. Microelectromech. Syst.* **12**, 160 (2003).

³M. Kurosawa, N. Kawabata, T. Sadoh, and M. Miyao, *Appl. Phys. Lett.* **95**, 132103 (2009).

⁴M. Scholz, M. Gjukic, and M. Stutzmann, *Appl. Phys. Lett.* **94**, 012108 (2009).

⁵Z. M. Wang, J. Y. Wang, L. P. H. Jeurgens, and E. J. Mittemeijer, *Phys. Rev. Lett.* **100**, 125503 (2008).

⁶Z. M. Wang, J. Y. Wang, L. P. H. Jeurgens, F. Phillipp, and E. J. Mittemeijer, *Acta Mater.* **56**, 5047 (2008).

⁷E. Pihan, A. Slaoui, and C. Maurice, *J. Cryst. Growth* **305**, 88 (2007).

⁸M. Kurosawa, Y. Tsumura, T. Sadoh, and M. Miyao, *Jpn. J. Appl. Phys.* **48**, 03B002 (2009).

⁹M. Gjukic, M. Buschbeck, R. Lechner, and M. Stutzmann, *Appl. Phys. Lett.* **85**, 2134 (2004).

¹⁰O. Nast and S. R. Wenham, *J. Appl. Phys.* **88**, 124 (2000).

¹¹Z. M. Wang, J. Y. Wang, L. P. H. Jeurgens, and E. J. Mittemeijer, *Phys. Rev. B* **77**, 045424 (2008).

¹²Z. M. Wang, L. P. H. Jeurgens, J. Y. Wang, and E. J. Mittemeijer, *Adv. Eng. Mater.* **11**, 131 (2009).

¹³F. Reichel, L. P. H. Jeurgens, and E. J. Mittemeijer, *Phys. Rev. B* **74**, 114103 (2006).

¹⁴Y. Du, Y. A. Chang, B. Y. Huang, W. P. Gong, Z. P. Jin, H. H. Xu, Z. H. Yuan, Y. Liu, Y. H. He, and F. Y. Xie, *Mater. Sci. Eng., A* **363**, 140 (2003).

¹⁵W. G. Pan, K. Fujiwara, N. Usami, T. Ujihara, K. Nakajima, and R. Shimokawa, *J. Appl. Phys.* **96**, 1238 (2004).

¹⁶C. C. Peng, C. K. Chung, and J. F. Lin, *J. Electrochem. Soc.* **157**, K260 (2010).

¹⁷J. H. Kim and J. Y. Lee, *Jpn. J. Appl. Phys.* **35**, 2052 (1996).

¹⁸M. S. Ashtikar and G. L. Sharma, *J. Appl. Phys.* **78**, 913 (1995).